INSTITUTE OF PHYSICS PUBLISHING BIOINSPIRATION & BIOMIMETICS

Bioinsp. Biomim. **1** (2006) S42–S48 doi:10.1088/1748-3182/1/4/S06

Passive cambering and flexible propulsors: cetacean flukes

Frank E Fish[1], **Moira K Nusbaum**[1], **John T Beneski**[1] **and Darlene R Ketten**[2]

[1] Department of Biology, West Chester University, West Chester, PA 19380, USA
[2] Biology Department, Woods Hole Oceanographic Institution, Woods Hole, MA 02543, USA

E-mail: ffish@wcupa.edu

Received 11 July 2006
Accepted for publication 11 September 2006
Published 22 December 2006
Online at stacks.iop.org/BB/1/S42

Abstract

The flukes are the primary locomotor structure in cetaceans, which produce hydrodynamic thrust as the caudal vertebrae are oscillated dorso-ventrally. Effective thrust generation is a function of the kinematics of the flukes, the angle of attack between the flukes and the incident water flow, and the shape of the flukes. We investigated the effect of bending within the caudal region of odontocete cetaceans to determine how changes in angular displacement between caudal vertebrae could effect passive shape change of the flukes. The internal and external changes of bent flukes were examined with computer tomography. Flukes and tailstock were removed from deceased *Delphinus delphis, Lagenorhynchus acutus*, *Peponocephala electra*, *Phocoena phocoena* and *Tursiops truncatus,* and bent on an adjustable support at 0, 45 and 90°. At 0°, cross-sections of the flukes displayed a symmetrical profile. Cross-sections of bent flukes (45°, 90°) were asymmetrical and showed a cambered profile. Maximum cambering occurred close to the tailstock and decreased toward the fluke tip. Maximum angular displacement occurred at the 'ball vertebra', which was located posterior of the anterior insertion of the flukes on the tailstock. Bending at the 'ball vertebra' passively cambers the flexible flukes. Cambering could increase hydrodynamic force production during swimming, particularly during direction reversal in the oscillatory cycle.

1. Introduction

Cetaceans (whales, dolphins, porpoises) swim by a high performance locomotor behavior in which the caudal flukes act as a hydrofoil to generate thrust. The oscillatory swimming motions incorporate dorso-ventral bending of the posterior third of the body in conjunction with pitching of the flukes, which follow a sinusoidal pathway (Fish 1998b). This locomotor pattern is categorized as carangiform with lunate-tail (thunniform) swimming and is typical of some of the fastest marine vertebrates, including scombrid fishes, lamnid sharks and cetaceans.

The flukes of cetaceans have been calculated to operate with high propulsive efficiency of 0.75–0.90 (Fish 1998b). This high efficiency surpasses most manufactured propellers, which have maximum efficiencies of 0.70 (Triantafyllou and Triantafyllou 1995). Furthermore, dolphins are able to adjust thrust production and efficiency by controlling the angle of attack of the oscillating flukes (Long *et al* 1997, Fish 1998a, 1998b). Angle of attack is defined as the angle between the tangent of the fluke's path and the axis of the fluke's chord. Maintenance of a positive angle of attack ensures thrust generation throughout the majority of the stroke cycle.

Rotating the flukes about a pitching axis allows for control of angle of attack. The rotation occurs at the base of the flukes, where there is a transition in the caudal vertebrae of the skeleton (Long *et al* 1997, Fish 1998b). As angle of attack is increased, lift will increase faster than the drag for a hydrofoil up to a critical level. Further increase of angle of attack leads to stalling with an increase in drag and precipitous loss of lift. Foils similar to whale flukes under steady flow conditions stall at angles of attack over 20°. However, an oscillating high aspect ratio fin can continue to generate lift, and thus thrust, up to an attack angle of 30° (Triantafyllou and Triantafyllou 1995). Conversely, at the top and bottom of the stroke, the flukes will have zero angle of attack as they rotate through the

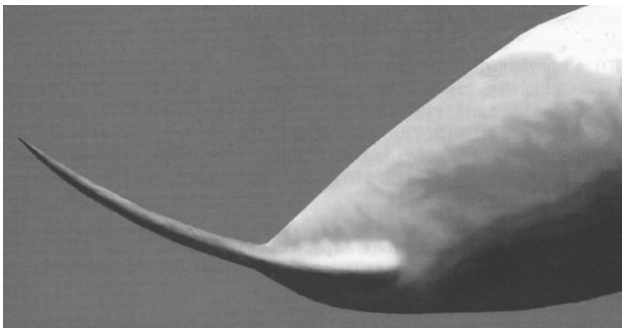

Figure 1. Lateral view of dolphin fluke from Romanenko (2002). The fluke is moving downward and is near the end of the down-stroke. There is a distinct curvature of the fluke from its insertion on the caudal peduncle to the fluke tip. Photograph was provided courtesy of Pensoft Publishers.

pitch axis and reverse direction. At these extreme positions, the flukes would have a zero angle of attack and potentially generate no thrust.

The hydrodynamic models, which were used to estimate thrust production and propulsive efficiency, considered the flukes as rigid hydrofoils (Parry 1949, Wu 1971, Lighthill 1975, Chopra and Kambe 1977, Fish 1993, 1998a, Lui and Bose 1993). These models did not account for the flexibility of the flukes, considering them rigid structures. The structural components of the flukes (i.e., collagen fibers) are not rigid and permit bending along the axes of the chord and span (figure 1, Joh (1925), Felts (1966), Purves (1969), Curren *et al* (1994), Romanenko (2002)). As structural and kinematic parameters determine locomotor performance, the flexible components of the dolphin flukes in conjunction with its propulsive oscillations are expected to enhance efficiency and energy economy (Alexander 1988, Pabst 1996). Flexibility across the chord can increase propulsive efficiency (Katz and Weihs 1978, Bose 1995). Katz and Weihs (1978) found the efficiency of an oscillating, flexible hydrofoil to increase by 20% with a small decrease in thrust, compared to a rigid propulsor executing similar movements. However, flexibility does not guarantee increased performance, as thrust was found to decrease slightly (Katz and Weihs 1978).

The flexibility of propulsive surfaces in cetaceans have not been detailed previously. For dolphins, flexibility in the flukes, particularly at the transitions of stroke cycle (i.e., as flukes change direction from upward to downward and *vice versa*), could maintain propulsive thrust continuously. Analyses were performed on changes in fluke geometry due to flexibility at transition. Medical computer tomography (CT) scans were made on isolated flukes to access three-dimensional changes in fluke structure due to bending. Bending of the flukes was expected to change the three-dimensional geometry of these structures and provide a shape, which potentially would enhance propulsion.

Figure 2. Planar views of representative flukes used in study. From top to bottom, the flukes examined are from Atlantic white-sided dolphin (*Lagenorhynchus acutus*), bottlenose dolphin (*Tursiops truncatus*), common dolphin (*Delphinus delphis*), harbor porpoise (*Phocoena phocoena*) and melon-headed whale (*Peponcephala electra*).

2. Methods

The flukes from five cetacean species (figure 2) were obtained from dead stranded animals collected by the New Jersey Marine Mammal Stranding Center (Brigantine, NJ). Choice of specimens to be examined was dependent on availability from strandings and size of the flukes that would fit through the portal of the CT scanner. Species included three common dolphin (*Delphinus delphis*), one Atlantic

Table 1. Morphometrics of flukes.

Species	*D. delphis*	*D. delphis*	*D. delphis*	*L. acutus*	*P. electra*	*P. phocoena*	*P. phocoena*	*T. truncatus*	*T. truncatus*	*T. truncatus*
Body length (m)	2.13	2.21	2.13	1.75	N/A	N/A	1.26	0.95	N/A	1.02
Body mass (kg)	N/A	113.4	76.2	42.2	N/A	N/A	N/A	10.9	N/A	15.0
Vertebrae in specimen	16	16	16	14	15	17	17	13	17	15
Vertebrae anterior to ball vertebra	8	8	7	4	4	8	10	4	8	7
Vertebrae posterior to ball vertebra	7	7	8	9	10	8	6	8	8	7
Fluke span (m)	0.46	0.51	0.44	0.36	0.65	0.26	0.30	0.21	0.30	0.24
Root chord (m)	0.15	0.15	0.14	0.14	0.19	0.098	0.11	0.11	0.12	0.12
Fluke area (m^2)	0.0458	0.0549	0.0431	0.0407	0.0805	0.0201	0.0242	0.0181	0.0267	0.0227
Aspect ratio	4.62	4.65	4.45	3.27	5.24	3.45	3.73	2.46	3.35	2.52

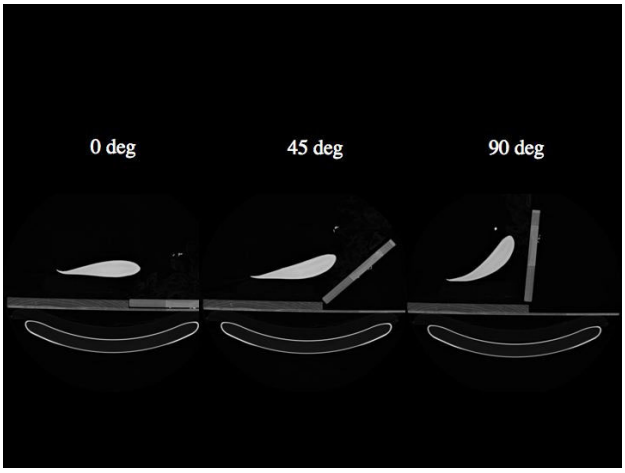

Figure 3. Cross-section of flukes from CT scans on an adjustable support. The flukes were scanned while flat (0°) and while bent at angles of 45° and 90°.

white-sided dolphin (*Lagenorhynchus acutus*), one melon-headed whale (*Peponcephala electra*), two harbor porpoises (*Phocoena phocoena*) and three bottlenose dolphins (*Tursiops truncatus*). Animals were transported to the University of Pennsylvania, School of Veterinary Medicine, New Bolton Center for necropsy. Flukes with tailstock were removed from the carcass, sealed in plastic bags, and subsequently frozen at −19 °C and stored at West Chester University.

Flukes remained frozen as they were transported to Woods Hole Oceanographic Institution for CT scanning. Prior to scanning the flukes were digitally photographed and allowed to thaw. Measurements on fluke dimensions using ImageJ (NIH version 1.3) included span (distance between fluke tips), root chord (distance from anterior insertion of fluke onto tail to trailing edge of fluke), and combined planar area (table 1). The aspect ratio of the flukes was calculated as the $\text{span}^2/\text{planar area}$. For scanning, flukes were laid flat on Styrofoam wedges on an adjustable support (figure 3). The support was constructed of two wooden boards. The boards were hinged together with thin rubber sheets glued to each board. The boards could lay flat (0°), or wooden blocks could be placed under one of the boards to produce angles of 45° and 90°. Such angles are representative of the angular deformations experienced by flukes during gliding (0°), swimming (45°) and tail-walking (90°) (Lang and Daybell 1963, Videler and Kamermans 1985, Fish 1998a). As expressed by standard deviation, variation in angular deflections of 0°, 45° and 90° was ±0.3°, 1.5° and 3.3°, respectively. The tailstock was attached to one board with elastic bands. The flukes were oriented so that the main bending axis (i.e., position of ball vertebra; Watson and Fordyce (1993), Tsai (1998)) was positioned over the board hinge. Flukes were oriented dorsal side up and scanned in the spanwise direction from fluke tip to tip. This orientation permitted images of cross-sections to be analyzed directly. Flukes were only bent in one direction as oscillations of the flukes during routine swimming follow a symmetrical sinusoidal pathway (Pyatetsky and Kayan 1975, Videler and Kamermans 1985, Goforth 1990, Fish 1993, 1998a, Fish and Rohr 1999).

CT scans were obtained with a Siemens Volume Zoom CT scanner at the Woods Hole Oceanographic Institution Ocean Imaging Center. Spiral protocols for data acquisition with 0.5 to 1 mm detector collimation at 1 mm s^{-1} table feeds were employed. All images were reconstructed in two formats (i.e., using conventional soft tissue and ultra-high kernels). Image reformats were provided as 512 matrix DICOM (Digital Imaging and Communications in Medicine format) outputs. A 10-fold expansion of the attenuation scale was applied to the data to improve discrimination of higher density components of structural elements as well as to eliminate artifacts from any potential metallic inclusions in the tissues. Images, in some instances, were reconstructed at 100 μ slice intervals to provide data based enhancements of the tissues under investigation. With these parameters, the maximum in-plane resolution was 0.35 mm at 2% of the modulation transfer function. This provided image data sets with isotropic 100 μ/side voxels. Prior studies suggest 25 μ in-plane pixel resolutions are possible, but a conservative nominal resolution is 50 μ.

Raw attenuation data were archived onto both CD and magneto-optical disks for all scans. Raw data were stored as a 1024 × 1024 attenuation matrix coded in 4096 levels of attenuation. Image files were produced in 512 × 512 matrices with attenuations compressed and represented visually as a 256 gray scale. Images were archived on disk also and printed as conventional CT films.

DICOM images of fluke cross-sections were examined every 10% of span from the central longitudinal axis of the tail

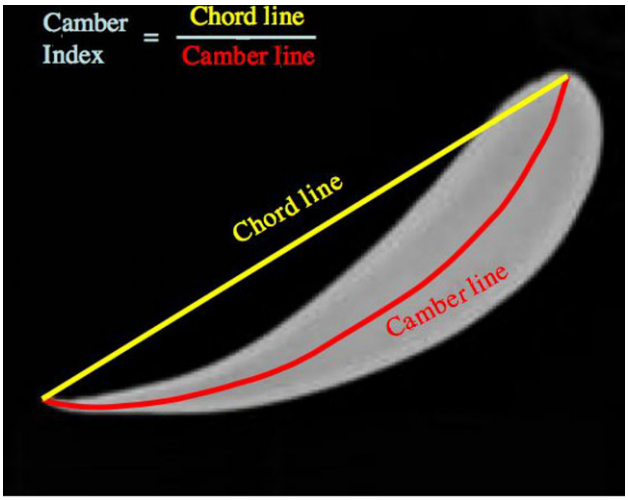

Figure 4. Fluke section from CT scan showing calculation of camber index from the chord line (white line) and camber line (black line).

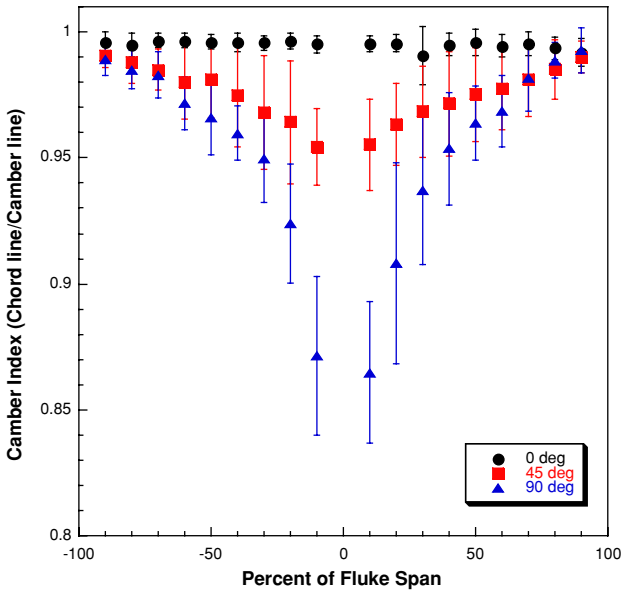

Figure 5. Mean values of camber index (±SD) as a function of per cent of fluke span for different experimental deflections (0°, 45°, 90°). The central axis of the tail is 0% and the fluke tip is 100%. Sections from the right fluke are indicated by negative span values and the left fluke with positive span values.

(0%) to the fluke tip (100%). Lengths of the camber line and chord line (figure 4) were determined using ImageJ software (NIH version 1.3) using the outline skeletonize algorithm after thresholding the image. The camber line is a curved line dividing the upper and lower surfaces of an airfoil. The chord line is a straight line connecting leading and trailing edges of the cross-section. A camber index was calculated as the length of the chord line divided by the length of the camber line. The chord line and camber line are the same for a symmetric foil section and give a camber index of unity.

Data were collected on the dimensions of a subset of the caudal vertebrae. Vertebrae height and length were measured from CT scans. As a complete set of caudal vertebrae was not imaged, vertebrae were numbered relative to the ball vertebra, where the ball vertebra was designated as zero and vertebrae posterior to it were positive integers and vertebrae anterior to it were negative integers. The ball vertebra was identified as a round or oval vertebra with convex cranial and caudal surfaces and no associated chevron bone (Rommel 1990, Tsai 1998). The inter-vertebral spacing between adjacent vertebrae was measured as the linear distance between the centers of the vertebral surfaces. To control for size, the intervertebral spacing was divided by the length of the vertebra immediately anterior to the spacing. Displacement angles of vertebrae were measured between the horizontal axis and the vertebral longitudinal axis.

Variation about means was expressed as ± one standard deviation (SD). As the camber index was a ratio, values were statistically analyzed after arcsine transformation to adjust for normality (Zar 1996). Simple repeated measured ANOVA was performed using SPSS (version 14.0; Chicago, IL) to evaluate the effect of fluke section on camber index. Sections were considered repeated measures of individuals that were not distinguished by species. The effect of vertebral number angle and spacing was not statistically analyzed, because vertebral number varied among individuals.

3. Results

A total of 11 540 cross-section images were imaged for the flukes of the ten specimens. Data from images were pooled for all specimens.

Cross-sections of flukes laid flat (0°) displayed a symmetrical profile (figure 5). The pooled camber index for sections of flukes lying flat was 0.99 ± 0.01. Repeated measures ANOVA of the arc-transformed camber index showed no significant difference among fluke sections for either right or left flukes ($F = 0.88$, d.f. $= 17$, $P = 0.598$). The sections had streamlined, fusiform profiles with a blunt and rounded leading edge and a thin, tapering trailing edge.

Static bending of the flukes at 45° and 90° showed a decrease in the camber index related to degree of bending and position in the fluke (figure 5, table 2). These changes in camber index were found to be statistically significant with repeated measures ANOVA (45°, $F = 11.03$, d.f. $= 17$, $P < 0.001$: 90°; $F = 52.64$, d.f. $= 17$, $P = 0.001$). The minimum camber index occurred at the root of the fluke at 10–20% of span. The pooled mean for minimum camber index was 0.96 ± 0.02 and 0.87 ± 0.03 at 45° and 90°, respectively. At 45°, *P. electra* and *L. acutus* had the highest and lowest minimum camber index, respectively; whereas at 90°, *P. phocoena* and *T. truncatus* had the highest and lowest values, respectively (table 2). camber index increased curvilinearly from the root of fluke to the fluke tip for both bending deflections of 45° and 90° (figure 5).

The largest length-specific intervertebral spacings were located about the ball vertebra (figure 6). The length-specific spacing anterior (intervertebral number −1) and posterior (intervertebral number 0) of the ball vertebra was 0.39 ± 0.20

Table 2. Camber index (±SD) listed by species for minimum value and value at 50% of span.

	Camber index minimum		Camber index 50% of span	
Species	45°	90°	45°	90°
Delphinus delphis	0.96 ± 0.02	0.87 ± 0.04	0.98 ± 0.01	0.98 ± 0.02
Lagenorhynchus acutus	0.94 ± 0.00	0.86 ± 0.00	0.98 ± 0.00	0.96 ± 0.01
Peponocephala electra	0.97 ± 0.01	0.87 ± 0.02	0.99 ± 0.00	0.97 ± 0.00
Phocoena phocoena	0.96 ± 0.02	0.87 ± 0.04	0.98 ± 0.01	0.98 ± 0.02
Tursiops truncatus	0.96 ± 0.01	0.85 ± 0.04	0.99 ± 0.01	0.96 ± 0.01

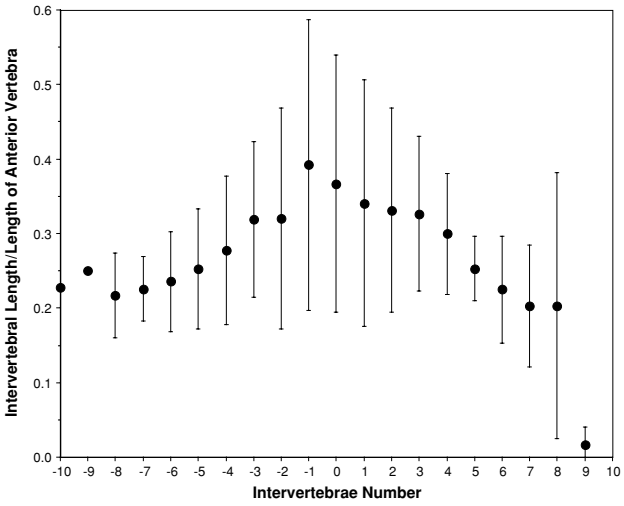

Figure 6. Mean values of scaled intervertebral length (±SD) as a function of intervertebral number.

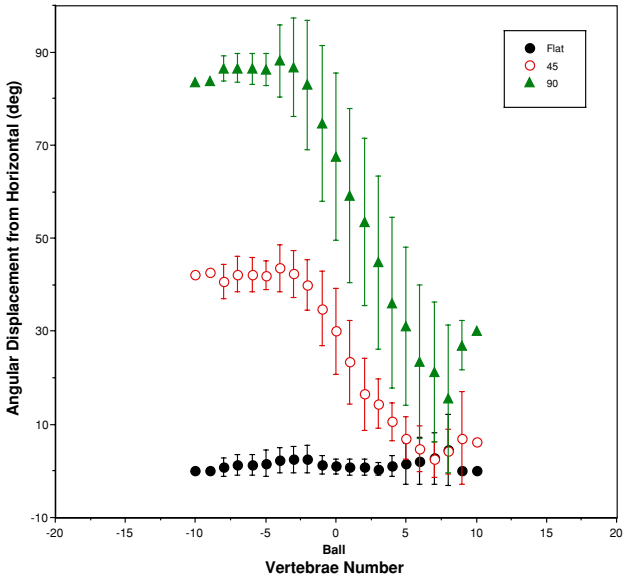

Figure 7. Mean values of angular displacement (±SD) from the horizontal for the longitudinal axis of each vertebra as a function of position in the vertebral column. Number 0 indicates the ball vertebra. Negative vertebral numbers are for vertebrae anterior of the ball vertebrae and positive numbers are for vertebrae posterior of the ball vertebra.

and 0.37 ± 0.17, respectively. The length-specific spacing decreased by 45–96% from the maximum value within ten intervertebral spaces anterior and posterior of the ball vertebra.

Angular displacement of the vertebrae increased with bending angle (figure 7). When the flukes were flat, the angular displacement for the pooled data had a mean angle of 1.62 ± 3.21°. This small displacement may have been a post-mortem artifact. When the flukes were statically bent at 45° and 90°, angular displacement decreased linearly from vertebrae −3 to 6 (figure 7). Large angular differences between adjacent vertebrae spanned the ball vertebra (vertebra number 0). At a 45° deflection, angular changes ranged from 4.77° to 6.68° between vertebrae −1 and 2; whereas at 90°, changes ranged from 5.68° to 8.75° between vertebrae −1 and 4. Vertebrae anterior to vertebra −3 generally maintained a constant angular displacement. Angular displacement for vertebrae posterior of vertebra 6 increased slightly.

4. Discussion

Flukes are flexible structures that permit chordwise bending. This flexibility is opposed to the simplified perception of flukes as rigid structures when analyzed in hydrodynamic models. Bending of the flukes can change the three-dimensional geometry of these structures. When no external load is provided, the flukes have symmetrical cross-sections along the span. However when statically bent, the flukes show varying degrees of cambering along the span. Camber is most extreme near the root. Cambering decreases toward the fluke tip.

Flexibility of the flukes is associated with their structural composition. The bulk of the flukes is composed of densely packed collagen fibers (Felts 1966, Miles 1998). An epidermis and subcutaneous blubber layer surround the fibrous core. The fibrous tissue is arranged in horizontal, vertical and oblique bundles (Felts 1966). Horizontal fibers radiate out through the fluke. The pattern of fiber bundles indicates an orientation appropriate for incurring high tensile stresses. Although flexible, this architecture would limit bending during the stroke cycle.

The flukes of swimming white-sided dolphin (*Lagenorhynchus acutus*) showed 35% and 13% deflections across the chord (i.e., distance from leading to trailing edges) and tip-to-tip span, respectively (Curren *et al* 1994). However, a swimming harbor porpoise displayed almost no bending at either the fluke tips or the trailing edge (Curren *et al* 1994). In the present study, camber was evident in the harbor porpoise (*P. phocoena*). Although compared with minimum value of

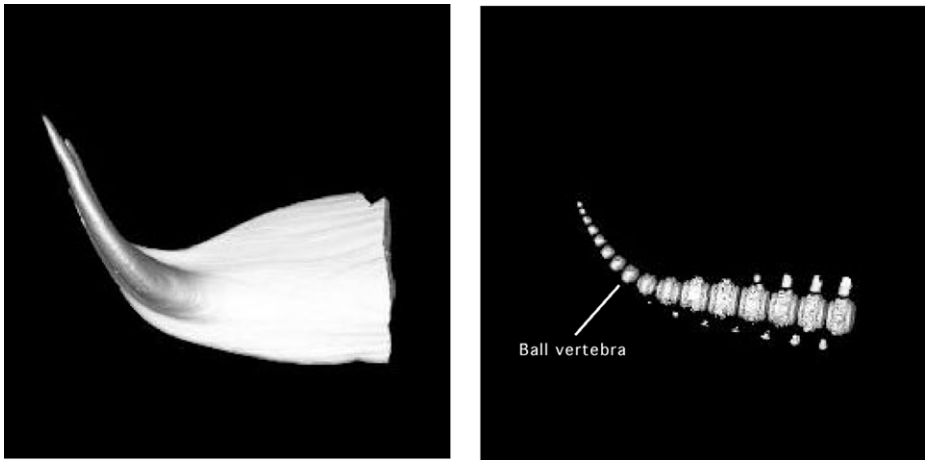

Figure 8. Three-dimensional reconstructions from CT scans of bent flukes (left) and of vertebral spine (right). Maximum bending coincides with position of rounded ball vertebra.

camber index for *L. acutus*, there was 0.6–3.6% and 3.1–4.3% less cambering at 45° and 90°, respectively. The lowest values of camber index were measured for *T. truncatus*. However, all three flukes from specimens of bottlenose dolphins (*T. truncatus*) were from neonatal dolphins. The flukes of neonates are less stiff than those of adults. Such differences in flexibility and cambering may reflect modification of the fibrous layers, which could affect swimming performance.

Flexibility across the chord can increase propulsive efficiency (Katz and Weihs 1978, 1979, Bose and Lien 1989, Prempraneerach *et al* 2003). A flexible foil can be cambered dynamically in accordance with local flow conditions (Liao 2004). Thus, cambering provides a favorable orientation of the foil to the incident flow in a time-dependent manner. Chordwise flexibility can increase efficiency by 20% with a small decrease in thrust, compared to a rigid propulsor executing similar oscillations (Katz and Weihs 1978). Propulsive efficiency for flexible foils reaches a maximum value for a range of Strouhal number of 0.2–0.35 (Prempraneerach *et al* 2003). This range of Strouhal number is in good agreement with the range for swimming cetaceans (Rohr and Fish 2004). The maximum propulsive efficiency for cetaceans occurs at Strouhal numbers between 0.25 and 0.35 (Rohr and Fish 2004).

The performance of rigid propellers is limited by the speed and frequency of movement. Standard rotation propellers, such as those found on boats, have a very limited range of operational speeds where efficiency is maximum (Fish and Lauder 2006). Above and below that optimal speed efficiency falls off precipitously (Breslin and Andersen 1994). The oscillating flukes of dolphins maintain a high efficiency of operation over a wide range of speeds without any sudden decrease in efficiency (Fish and Lauder 2006).

Cambering throughout the stroke could provide increased lift and thrust production. Cambering would be beneficial to maintain lift production at the end of each stroke as the flukes change direction. If the flukes were straight and rigid, there is a period of feathering (i.e., chord line parallel to the incident flow), which would generate no thrust and reduce efficiency. Cambering would potentially allow the flukes to maintain thrust production through the change in oscillation direction. Furthermore, a smoother transition due to flexibility can allow the flukes to operate without stalling. Indeed, Romanenko (2002) showed that curvature of the flukes increased more at the lowermost position of the down-stroke compared to the middle of the stroke. The calculated camber index was 0.94 and 0.98 at the end and middle of the down-stroke, respectively, for *T. truncatus* swimming at routine speeds (figures 6.6 and 6.7 from Romanenko (2002)).

Maximum flexion in the tail occurs near the base of the flukes at a vertebra known as the 'ball vertebra' (Watson and Fordyce 1993, Tsai 1998). This vertebra has convex (rounded) anterior and posterior faces and differs from the other vertebrae, which have flat faces. The location of the ball vertebra with respect to attachment of the flukes on the tailstock determines the passive deformation of the flukes into a cambered structure. The ball vertebra is posterior of the forward insertion of the flukes on the tailstock (figure 8). Flexion around the ball vertebra posterior of the anterior insertion causes a smooth bending of the flukes in the chordwise direction. The ability to rotate the flukes about a pitching axis at the ball vertebra allows for control of angle of attack when swimming (Long *et al* 1997, Fish 1998b). Cambering, thus, is a consequence of pitch control at the base of the flukes to maintain thrust production.

As exhibited by the flukes of cetaceans, flexibility and its associated cambering may provide an alternate or superior solution to propulsion involving rotational or oscillating, engineered propellers. There is considerable naval interest in dolphin locomotion as the basis for the development of high efficiency propulsors in the construction of undersea vehicles (Saunders 1951, Fish and Rohr 1999, Bandyopadhyay 2002).

Acknowledgments

The research was funded by grants to FEF from the Office of Naval Research (N00014-02-1-0046; Program manager

Promode Bandyopadhyay) and the West Chester University College of Arts and Sciences Development Award. We are grateful to the assistance of Julie Arruda, Win Fairchild, Perry Habecker, Scott Kramer, Jennifer Maresh and Robert Scholkoff. Flukes were collected with permission of the Northeast regional office of the National Marine Fisheries Service.

References

Alexander R McN 1988 *Elastic Mechanisms in Animal Movement* (Cambridge: Cambridge University Press)

Bandyopadhyay P R 2002 A biomimetic propulsor for active noise control: experiments *NUWC-NPT Technical Report 11351* (Newport, RI: Naval Undersea Warfare Center)

Bose N 1995 Performance of chordwise flexible oscillating propulsors using a time-domain panel method *Int. Shipbuild. Prog.* **42** 281–94

Bose N and Lien J 1989 Propulsion of a fin whale (*Balaenoptera physalus*): why the fin whale is a fast swimmer *Proc. R. Soc.* B **237** 175–200

Breslin J P and Andersen P 1994 *Hydrodynamics of Ship Propellers* (Cambridge: Cambridge University Press)

Chopra M G and Kambe T 1977 Hydrodynamics of lunate-tail swimming propulsion: part 2 *J. Fluid Mech.* **79** 49–69

Curren K C, Bose N and Lien J 1994 Swimming kinematics of a harbor porpoise (*Phocoena phocoena*) and an Atlantic white-sided dolphin (*Lagenorhynchus acutus*) *Mar. Mamm. Sci.* **10** 485–92

Felts W J L 1966 Some functional and structural characteristics of cetacean flippers and flukes *Whales, Dolphins, and Porpoises* ed K S Norris (Berkeley, CA: University of California Press) pp 255–76

Fish F E 1993 Power output and propulsive efficiency of swimming bottlenose dolphins (*Tursiops truncates*) *J. Exp. Biol.* **185** 179–93

Fish F E 1998a Comparative kinematics and hydrodynamics of odontocete cetaceans: morphological and ecological correlates with swimming performance *J. Exp. Biol.* **201** 2867–77

Fish F E 1998b Biomechanical perspective on the origin of cetacean flukes *The Emergence of Whales: Evolutionary Patterns in the Origin of Cetacea* ed J G M Thewissen (New York: Plenum) pp 303–24

Fish F E and Lauder G V 2006 Passive and active flow control by swimming fishes and mammals *Ann. Rev. Fluid Mech.* **38** 193–224

Fish F E and Rohr J 1999 Review of dolphin hydrodynamics and swimming performance *SPAWARS System Center Technical Report 1801 (San Diego, CA)*

Goforth H W 1990 Ergometry (exercise training) of the bottlenose dolphin *The Bottlenose Dolphin* ed S Leatherwood and R R Reeves (San Diego, CA: Academic) pp 559–74

Hamilton J L, McLellan W A and Pabst D A 1998 Functional morphology of harbor porpoise (*Phocoena phocoena*) tailstock blubber *Am. Zool.* **38** 203A

Joh C G 1925 The motion of whales during swimming *Nature* **116** 327–9

Katz J and Weihs D 1978 Hydrodynamic propulsion by large amplitude oscillation of an airfoil with chordwise flexibility *J. Fluid Mech.* **88** 485–97

Katz J and Weihs D 1979 Large amplitude unsteady motion of a flexible slender propulsor *J. Fluid Mech.* **90** 713–23

Kayan V P 1979 The hydrodynamic characteristics of the caudal fin of the dolphin *Bionika* **13** 9–15 (translated from Russian)

Lang T G and Daybell D A 1963 Porpoise performance tests in a seawater tank *Nav. Ord. Test Sta. Tech. Rep.* p 3063 (China Lake, CA)

Liao J C 2004 Neuromuscular control of trout swimming in a vortex street: implications for energy economy during the Kármán gait *J. Exp. Biol.* **207** 3495–506

Lighthill J 1975 *Mathematical Biofluiddynamics* (Philadelphia, PA: Soc. Ind. Appl. Math.)

Liu P and Bose N 1993 Propulsive performance of three naturally occurring oscillating propeller planforms *Ocean Eng.* **20** 57–75

Liu P and Bose N 1997 Propulsive performance from oscillating propulsors with spanwise flexibility *Proc. R. Soc.* A **453** 1763–70

Liu P and Bose N 1999 Hydrodynamic characteristics of a lunate shape oscillating propulsor *Ocean Eng.* **26** 519–29

Long J H Jr, Pabst D A, Shepherd W R and McLellan W A 1997 Locomotor design of dolphin vertebral columns: bending mechanics and morphology of *Delphinus delphis J. Exp. Biol.* **200** 65–81

Miles L E C 1998 Structure and function in cetacean and sirenian flukes *Honors Thesis* Department of Anatomy and Human Biology (Perth, WA: The University of Western Australia)

Pabst D A 1996 Springs in swimming animals *Am. Zool.* **36** 723–35

Pabst D A, Hamilton J L, McLellan W A, Williams T M and Gosline J M 1999a Streamlining dolphins: designing soft-tissue keels *Proc. 11th Int. Symp. on Unmanned, Untethered Submersible Technology* (Lee, NH: Autonomous Undersea Systems Institute)

Pabst D A, McLellan W A and Williams T M 1999b Locomotor functions of dolphin blubber *Am. Zool.* **39** 114A

Parry D A 1949a The swimming of whales and a discussion of Gray's paradox *J. Exp. Biol.* **26** 24–34

Parry D A 1949b Anatomical basis of swimming in whales *Proc. Zool. Soc. Lond.* **119** 49–60

Prempraneerach P, Hover F S and Triantafyllou M S 2003 The effect of chordwise flexibility on the thrust and efficiency of a flapping foil *Proc. 13th Int. Symp. on Unmanned Untethered Submersible Technology: Proc. Special Session on Bio-Engineering Research Related to Autonomous Underwater Vehicles* (Lee, NH: Autonomous Undersea Systems Institute)

Purves P E 1969 The structure of the flukes in relation to laminar flow in cetaceans *Z. Säugertierkunde* **34** 1–8

Pyatetsky V Ye and Kayan V P 1975 On kinematics of swimming bottlenose dolphin *Bionika* **9** 41–5 (translated from Russian)

Rohr J J and Fish F E 2004 Strouhal numbers and optimization of swimming by odontocete cetaceans *J. Exp. Biol.* **207** 1633–42

Romanenko E V 2002 *Fish and Dolphin Swimming* (Sofia: Pensoft)

Rommel S 1990 Osteology of the bottlenose dolphin *The Bottlenose Dolphin* ed S Leatherwood and R R Reeves (San Diego, CA: Academic) pp 29–49

Saunders H E 1951 Some interesting aspects of fish propulsion *Soc. Nav. Arch. Mar. Eng., Ches. Sect.* **3 May 1951**

Triantafyllou G S and Triantafyllou M S 1995 An efficient swimming machine *Sci. Am.* **272** 64–70

Tsai W-L 1998 Dorsoventral bending of the tail and functional morphology of the caudal vertebrae in the bottlenose dolphin, *Tursiops truncatus Master's Thesis* (Stillwater, OK: Oklahoma State University)

Videler J and Kamermans P 1985 Differences between upstroke and downstroke in swimming dolphins *J. Exp. Biol.* **119** 265–74

Watson A G and Fordyce R E 1993 Skeleton of two minke whales, *Balaenoptera acutorostrata*, stranded on the south-east coast of New Zealand *New Zealand Nat. Sci.* **20** 1–14

Wu T Y 1971 Hydrodynamics of swimming propulsion. Part 2. Some optimum shape problems *J. Fluid Mech.* **46** 521–544

Zar J H 1996 *Biostatistical Analysis* (Upper Saddle River, NJ: Prentice-Hall)